The following manuscript was accepted for publication in Pharmaceutical Sciences. It is assigned to an issue after technical editing, formatting for publication and author proofing
Citation: Fandiño OE, FBruno FP, Monti GA, Sperandeoa NR. Mechanochemical synthesis of a novel eutectic of the antimicrobial nitazoxanide with improved dissolution performance, Pharm Sci. 2021, doi: 10.34172/PS.2021.10

Mechanochemical synthesis of a novel eutectic of the antimicrobial nitazoxanide with improved dissolution performance

Octavio E. Fandiño,[a] Flavia P. Bruno,[b,1] Gustavo A. Monti,[c] Norma R. Sperandeo[a*]

[a] Universidad Nacional de Córdoba. Facultad de Ciencias Químicas. Departamento de Ciencias Farmacéuticas y Unidad de Investigación y Desarrollo en Tecnología Farmacéutica (UNITEFA)-CONICET, Ciudad Universitaria, X5000HUA Córdoba, Argentina.

[b] Universidad Nacional de Córdoba, Facultad de Ciencias Químicas. Departamento de Ciencias Farmacéuticas, Haya de la Torre y Medina Allende, Ciudad Universitaria, X5000HUA, Córdoba, Argentina.

[c] Universidad Nacional de Córdoba. Facultad de Astronomía, Matemática, Física y Computación y IFEG-CONICET, Ciudad Universitaria, X5000HUA Córdoba, Argentina

Corresponding author: Norma R. Sperandeo. E-mail: norma.sperandeo@unc.edu.ar (N.R.S); http://orcid.org/0000-0002-2380-6328

---

[1]Present address: Laboratorio Fresenius Kabi, Del Comercio 757, X5016JSA Córdoba, Argentina.

Abstract

Background: Nitazoxanide (NTZ) is a broad spectrum antimicrobial agent with poor aqueous solubility and low bioavailability. Thus, the generation of new solid forms of NTZ is relevant to improve its unfavorable properties. The present study deals with the application of mechanochemistry for the preparation of alternate solid forms of NTZ, using saccharine (SAC) as coformer.

Methods: NTZ-SAC mixtures were prepared by neat and liquid-assisted grinding (LAG) and characterized using differential scanning calorimetry (DSC), hot stage microscopy (HSM), X-ray Powder Diffraction (XRPD), ^{13}C Solid-state Nuclear Magnetic Resonance (SSNMR) and Diffuse Reflectance Infrared Fourier Transform (DRIFT) spectroscopy. Powder dissolution (PD) profiles were obtained with USP apparatus 2 in buffer phosphate pH 6.5 with 0.25% Tween® 80 - 0.25% triethanolamine and in 0.25% sodium lauryl sulfate, at 37 ºC ± 0.5 ºC and 75 rpm. Drug release was characterized in terms of dissolution efficiency (DE).

Results: XRPD, SSNMR and DRIFT indicated that NTZ and SAC did not cocrystallize but DSC and HSM revealed that they formed a binary eutectic mixture which melted near 176 °C, a melting temperature lower than those of NTZ and SAC. PD data indicated that the 1:1 NTZ-SAC sample obtained by LAG exhibited a slightly higher DE than pure NTZ in the two assayed media.

***Conclusion*:** NTZ and SAC formed a eutectic, the first reported for this drug, which improved its dissolution rate and opened the pathway for studies searching for new eutectics with better biopharmaceutical attributes than NTZ and the NTZ-SAC eutectic reported herein.

Keywords: differential scanning calorimetry; dissolution efficiency; powder dissolution; liquid-assisted grinding; saccharine, X-ray powder diffraction.

Introduction

Nitazoxanide [2-(acetyloxy)-*N*-(5-nitro-2-thiazolyl)benzamide, NTZ] (Figure 1) is a nitrothiazole derivative used in the treatment of diarrhea caused by *Cryptosporidium parvum* and *Giardia intestinalis* in adults and children at least 12 months of age.[1] NTZ is also active against numerous other parasitic pathogens and viruses, including *Trypanosoma cruzi* (the causative agent of American trypanosomiasis),[2] *Leishmania mexicana*,[2] the ulcer-causing pathogen *Helicobacter pylori*,[3] multidrug resistant strains of *Mycobacterium tuberculosis*,[1] as well as respiratory viruses, rotavirus, norovirus, coronavirus, hepatitis B and C, dengue-2, yellow fever, Japanese encephalitis, and human immunodeficiency viruses.[4] Moreover, NTZ has shown anticancer activity,[4] and is a promising compound for the treatment of neuropathic pain,[4] the Ebola virus disease[4] and is also under investigation for potential use in COVID-19 treatment.[5]

Although NTZ is an agent with diverse pharmacological activities and minimal toxicity, it has unfavorable physicochemical and biopharmaceutical properties, in particular very poor aqueous solubility[6] and low bioavailability,[4] and this provided the motivation for discovering new solid forms which may improve its solubility, dissolution rate, and bioavailability, and thus provide improved therapeutic options for patients. In fact, **NTZ** has been in the focus of pharmaceutical research to discover and prepare alternative solid forms such as cyclodextrin complexes,[7,8] solid dispersions,[9] cocrystals[10] and cocrystal alloys.[11] Regarding NTZ cocrystals, it was found that it cocrystallized with five organic acids [succinic,[10] glutaric,[10] 2,5-dihydroxybenzoic,[10] *p*-aminobenzoic and *p*-aminosalicylic[11]], showing a common heterodimeric synthon formed between the carboxyl group of the acid coformer and the carboxamidine group of NTZ (Figure 1), namely the carboxyl-carboxamidine synthon.[10,11]

Pursuing our interest in discovering new solid forms of NTZ, the aim of this study was to determine if NTZ can be partnered with a non-carboxylic acid coformer such as saccharine (SAC, pKa = 2.2[12], Figure 1) which cannot form the above-mentioned carboxyl-carboxamidine synthon with NTZ, but is able to generate N–H···O, S=O··H–N, O-H-O and N-H-N hydrogen bonds with drugs possessing OH, NH or carbonyl groups[12,13] such as NTZ, leading to cocrystals, salts or eutectics, with the last representing a whole new paradigm of noncovalent derivatives[14] and technology at par with other crystal engineering techniques in improving clinically significant attributes of a drug[14] such as solubility, stability, and bioavailability, as demonstrated for curcurmin,[15] hesperetin,[14] and leflunomide.[16]

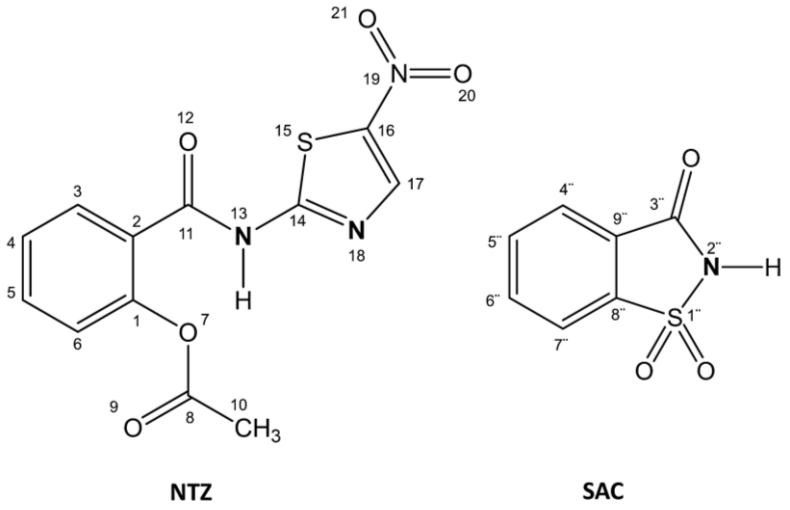

Figure 1. Schemes of the molecules of nitazoxanide (NTZ) and saccharine (SAC), and atom numbering used in the SS ^{13}C NMR study for NTZ and SAC.

In effect, depending upon various factors, during cocrystallization, an amalgamation of two complementary interacting materials lead to the formation of a specific product which can be any of the multicomponent organic adduct (solvate, molecular salt, eutectic or a cocrystal).[16] The formation of either cocrystal or eutectic during cocrystallization is mutually exclusive and a win-win situation.[16] According to Cherukuvada and Nangia,[17] the materials with strong adhesive (hetero) interactions between the unlike components will lead to cocrystals whereas those having

stronger cohesive (homo/self) interactions will more often give rise to solid solutions (for similar structures of components) and eutectics (for different structures of components). In case of a eutectic, the adhesive (heteromolecular) interactions are relatively weaker as they are formed between non-isomorphous materials (having size/shape mismatch between the components), the structure lacks a unique lattice arrangement distinct from the individual components and retains the cohesive interactions in its solid solutions.[17] In comparison, a cocrystal is formed when the adhesive interactions can overcome the size/shape mismatch features of the components, and the resultant crystal packing is distinct from the parent components.[17]

This article deals with the experimental details in which attempts to form cocrystals of NTZ with SAC by using mechanochemical grinding led to eutectic formation, thus revealing NTZ-SAC to be a eutectic-forming system.

Materials and Methods

Chemicals

Nitazoxanide raw powder was isolated from Nixoran® suspension (Roemmers, Argentine) by solvent extraction and purified by recrystallization from ethyl acetate. SAC was commercially acquired and purified by crystallization from ethanol-water. Spectral grade KBr (Merck, Argentina), filter paper (2.7 μm, Whatman 542, UK) and nylon membranes (0.45 μm, Pall Corporation, USA) were commercially acquired. Water was obtained from a Milli-Q water purification system (Millipore, Bedford, MA, USA). *o*-Phosphoric acid (85% v/v) was purchased from Cicarelli® Laboratorios (Reagents S.A., Argentina). All the other solvents used were of analytical or HPLC grade and obtained from commercial suppliers.

Mechanochemical synthesis

The syntheses were performed using neat grinding (NG)[18,19] and liquid-assisted grinding (LAG)[18-20] methods. Briefly, NTZ and SAC (both as powders) were mixed in 1:1, 1:2 and 2:1 stoichiometric ratios and manually ground in an agate mortar with a pestle for 20 min without adding solvent (NG) or adding a few drops of acetone (LAG). In what follows, the samples obtained by using NG and LAG will be coded as NTZ-SAC_{NG} and NTZ-SAC_{LAG}, respectively.

Binary mixtures (in ratios of 80/20, 60/40, 50/50, 40/60 and 20/80, w/w) were also prepared by gently mixing accurately weighed amounts of NTZ and SAC (both as powders) in an agate mortar with pestle for 3 min. The resulting samples were stored under vacuum (over $CaCl_2$) until analyzed.

The preliminary characterization of the obtained samples was made by using hot-stage microscopy, and their melting points and behavior on heating were compared with those of the pure components. On the basis of the results obtained, selected samples were also characterized using diffractometric, vibrational and thermal techniques.

X-ray Powder Diffraction

XRPD patterns were collected at 23–25 °C on a Philips X´Pert PRO PANalytical powder diffractometer (Philips, The Netherlands), fitted with a Copper tube (CuKα = 1.54178 Å) and a Ni filter, with the X-ray generator being set at a voltage of 40 kV and a current of 30 mA. Samples were analyzed with a step size of 0.05° 2θ and a step time of 3 s from 3 to 35° 2θ, using a 25 mm diameter Si single-crystal holder.

Diffuse reflectance infrared Fourier transform

DRIFT spectra were recorded on a Nicolet Avatar 360 FTIR spectrometer (Nicolet Instruments Corp., Madison, WI), using a diffuse reflectance accessory and macro diffuse reflectance cups of 13 mm diameter (~400 mg capacity). For the preparation of the sample-KBr blend, dry KBr was

ground for 2 min before mixing with the sample (5 % w/w) in an agate mortar with only light grinding performed. The blend was then placed in the cup, and excess material was removed by placement of a microscope slide against the open cup in a rotary motion to achieve a level but roughened surface, which was scanned immediately. KBr scans were used as background. Spectra were acquired by accumulating 64 scans at 4 cm^{-1} resolution. All spectra were processed using the OMNIC E.S.P. 5.1 program (Nicolet Corp.).

Differential scanning calorimetry (DSC), hot-stage microscopy (HSM) and melting point determination

DSC measurements were performed on a MDSC 2920 analyzer (TA Instruments Inc., USA) at a heating rate of 10 °C/min under N_2 (99.99% purity, flow rate 50 mL/min). The temperature axis was calibrated with indium (99.99% purity, *m.p.* 156.6 °C). Non hermetically-closed aluminum pans (40 μL) were used. Samples with a mass of 1-2 mg were employed. Empty aluminum pans were used as references. Data were treated with the Universal Analysis 2000 software (TA Instruments Inc.).

The physical and morphological changes that occurred during the process of heating of solid samples were observed through a microscope fitted with a Kofler hot-stage (Leitz, Wetzlar, Germany) at a constant rate of about 8 °C/min

Melting point (*m.p.)* determinations were also made on an IA9100 Electrothermal digital melting point apparatus (Cole-Parmer Ltd., United Kingdom).

NMR spectroscopy

^{13}C SSNMR studies were performed using the ramp CPMAS sequence with proton decoupling during acquisition, at 25 °C in a Bruker Avance II 300 spectrometer (Bruker, Germany), operating frequency for carbons 75 MHz, equipped with a 4 mm MAS probe. Spinning rate was

8 kHz. The recycling time was 20 s, the contact time during CP was 2 ms, and 2048 scans were recorded. TPPM15 sequence was used for decoupling during acquisition with a proton field H_{1H} satisfying $\omega_{1H}/2\pi = \gamma_H H_{1H}/2\pi = 50.0$ kHz. Chemical shifts were quoted with respect to tetramethylsilane (TMS) and measured via replacement with adamantane (29.50 and 38.56 ppm). Interrupted decoupled experiments were conducted using a 40 μs delay before acquisition. The signal assignments of the spectra were achieved by dipolar dephasing experiments [which yields quaternary carbons only and the corresponding non-quaternary suppression (NQS) spectrum] and by comparison with reported SS NMR data for NTZ[21] and SAC.[22,23]

Powder dissolution study

Dissolution experiments were conducted under non-sink conditions on an USP paddle apparatus (Apparatus 2), using a Sotax AT7 Smart semi-automated dissolution tester (Sotax Corp. Horsham, Pennsylvania, USA), 500 mL of dissolution medium, 37 °C ± 0.5 °C and 75 rpm. The dissolution media were (a) buffer phosphate pH 6.5 with 0.25% (w/v) Tween® 80 and 0.25% (w/v) triethanolamine (named hereafter as Tween®-t), which is a simplified biorrelevant medium for poorly water-soluble compounds that simulates small intestinal conditions,[24] and (b) 0.25% (w/v) sodium lauryl sulfate (SLS) in MilliQ water. Accurately weighed powdered samples (sieved through a 100 mesh screen) containing 40 mg of pure NTZ or the equivalent of 40 mg of NTZ eutectic were rapidly tipped from aluminum boats onto the stirred dissolution medium. The volume of media and sample masses used were selected taking into account the level of quantitation of NTZ using the HPLC method of Malesuik et al.,[25] which we described below, and the solubility of NTZ in Tween®-t and SLS at 37 ºC, which we found to be 26 μg/mL (Tween®-t) and 12 μg/mL (SLS). With 40 mg of NTZ and a test volume of 500 mL, sink conditions did not prevail neither in Tween®-t nor in SLS since the tests volumes were not at least greater than three times those required to form a saturated solution,[26] but the tests

volumes allowed quantification above the limit of quantitation of NTZ (0.4 μg/mL[25]). For all experiments, samples (3 mL) were withdrawn at time intervals of 5, 10, 15, 30, and 45 min, and immediately filtered (0.45 μm nylon membrane). In all cases, the first milliliter was discarded. Filtered aliquots were then diluted with mobile phase and assayed by HPLC.

Chromatographic separations were achieved using an HPLC chromatograph (AGILENT® S1100, 20 μL fixed loop injector [Agilent 1100 G-1313A] and variable UV-Visible detector [Agilent G1365B]), using a previously reported validated method that uses an isocratic mode; 20-25 °C; *o*-phosphoric acid (0.1%, v/v, pH 6.0, adjusted by addition of triethylamine)-acetonitrile (45:55, v/v), filtered (0.45 μm) and degassed using vacuum; Synergi-4m-Fusion RP-80 C18 (Phenomenex, 250mm x 4.6 mm, 4.5 μm) column and UV-visible detection at 240 nm.[25] The amount of dissolved NTZ was calculated by reference to a standard calibration curve constructed using five concentration levels of NTZ (r^2 = 0.9997). An accumulative correction was made in order to compensate for previously removed samples. Peak areas were integrated using the program Chemstation Rev. A.10.02 for Windows.

Dissolution profiles were represented as the cumulative percentages of the amount of drug released at each sampling interval, with the profiles in Tween®-t and SLS being the average of three and two individual powdered samples, respectively. Dissolution profiles were characterized in terms of dissolution efficiency (DE). This model independent parameter is defined as the area under the dissolution curve up to a certain time, *t*, expressed as a percentage of the area of the rectangle described by 100% dissolution in the same time.[27] DE was calculated from the area under the curve (measured using the trapezoidal rule) at the last sample time point (45 min) and expressed as a percentage of the area of the rectangle described by 100% dissolution at the same time.

Results and discussion

XRPD, SSNMR, DRIFT and DSC data

NTZ was subjected to mechanochemical grinding with SAC, with and without solvent, in the intent of obtaining multicomponent adducts. The resultant samples were white solids, like pure NTZ and SAC (Figure S1), and were initially examined by means of HSM for morphology and behavior on heating. According to HSM observations, all the obtained samples were cryptocrystalline solids that exhibited similar behavior on heating, namely a fusion process at about 175 °C, a gradual decomposition above 180 °C and the melting with decomposition of remaining solid particles (excess starting compounds). The HSM images of the 1:1 NTZ-SAC samples obtained by NG and LAG (taken as representative of NTZ-SAC products), together with those of NTZ and SAC, are depicted in Figures S2-S5. Thus, taking into account that XRPD is a diagnostic way of differentiating cocrystalline phases from physical mixtures/eutectics,[28] the XRPD patterns of the prepared samples were recorded. Figure 2 exhibits the powder patterns of NTZ, SAC, their 1:1 physical mixture (1:1 PM) and three NTZ-SAC products. As shown in Figure 2, the XRPD patterns of the three NTZ-SAC products are the superposition of those of NTZ and SAC, like their respective 1:1 PM, indicating that the three samples represent physical mixtures or eutectics.

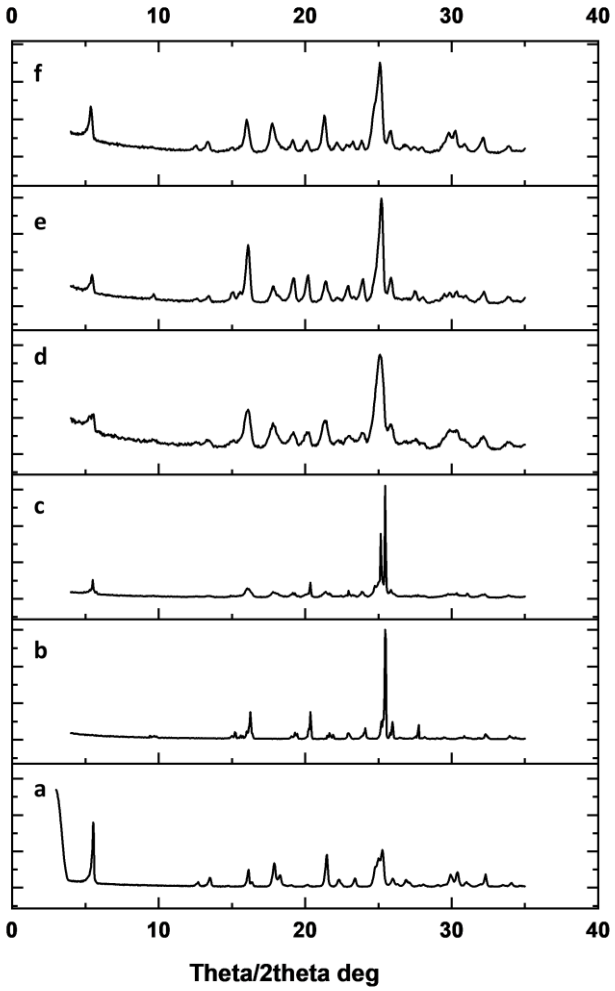

Figure 2. X-ray powder diffraction patterns of (a) NTZ; (b) SAC; (c) 1:1 PM; (d) 1:1 NTZ-SAC_{LAG}; (e) 1:2 NTZ-SAC_{LAG}, and (f) 2:1 NTZ-SAC_{LAG}.

In order to characterize further the NTZ-SAC products, SSNMR and DRIFT were used since both techniques are powerful tools for characterizing materials and can confirm or discard an interaction between molecules. The ^{13}C CP/MAS spectra of the 1:1 PM and two NTZ-SAC products, together with those of their starting compounds, are depicted in Figure 3, while the chemical shift values are listed in Table S1. The DRIFT spectra of NTZ, SAC and representative NTZ-SAC products are shown in Figure S6.

As shown in Figure 3, the spectra of 1:1 NTZ-SAC_{NG} (Figure 3d) and 1:2 NTZ-SAC_{LAG} (Figure 3e) correspond to the sum of the spectra of the reagents (Figure 3a,b), like the 1:1 PM

(Figure 3c), indicating the absence of phases with new molecular arrangement in the lattices. Only the carbonyl carbon of pure SAC (C3´, Table S1) observed at 163.8 ppm was slightly shifted to 162.9 (1:1 PM), 163.0 (1:1 NTZ-SAC_{NG}) and 163.6 (1:2 NTZ-SAC_{LAG}) ppm, but these shifts were not significant.

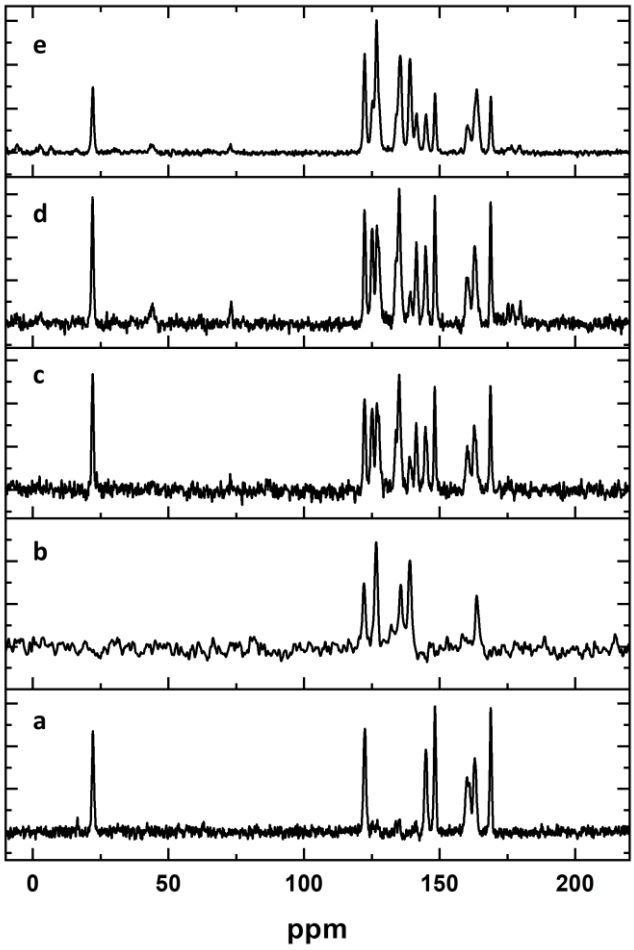

Figure 3. ^{13}C CPMAS NMR spectra of (a) NTZ; (b) SAC; (c) 1:1 PM; (d) 1:1 NTZ-SACNG, and (e) 1:2 NTZ-SACLAG.

The DRIFT spectra of the 1:1 NTZ-SAC_{NG}, 1:1 NTZ-SAC_{LAG}; 1:2 NTZ-SAC_{NG} and 1:2 NTZ-SAC_{LAG} samples (Figure S6) were also the superposition of those of the respective starting materials, like their 1:1 PM (Figure S6), indicating that all samples represent physical mixtures or eutectics, in accordance with the XRPD and SSNMR evidence. Hence, since DSC works as a

bench diagnostic technique for a eutectic and cocrystals,[28,29] the behavior on heating of the obtained samples was assessed by DSC.

The DSC curves of NTZ and SAC (Figure 4a,b) displayed, in the 25-250 °C temperature range, sharp melting endotherms with extrapolated onset temperatures (Te) of 201.1 °C (NTZ, Figure 4a) and 227.8 °C (SAC, Figure 4b). It should be noted that both compounds are stable on heating as solids but as liquids are unstable to undergo thermal decomposition reactions,[21,23] and this precluded the determination of their binary solid–liquid phase diagram by classical methods of melting of mixtures and their solidification.[30]

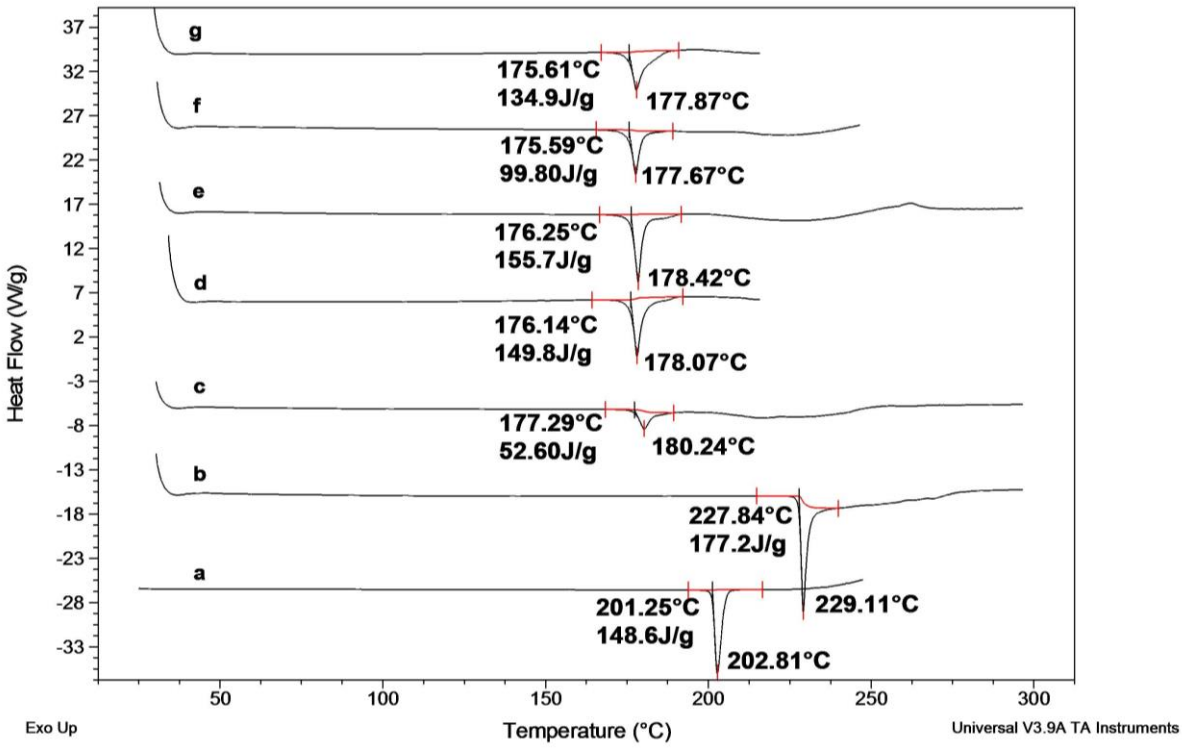

Figure 4. DSC (non-hermetically sealed aluminum pans, β = 10 °C/min and N_2 purge of 50 mL/min) of (a) NTZ; (b) SAC; (c) 1:1 PM; (d) 1:1 NTZ-SAC_{NG}; (e) 1:2 NTZ-SAC_{NG}; (f) 1:2 NTZ-SAC_{LAG}, and (g) 2:1 NTZ-SAC_{NG}.

The DSC scans of the 1:1 PM (Figure 4c) and those of three representative NTZ-SAC samples (Figure 4d-f) exhibited, in the 25-200 °C temperature range, single endotherms near to 176 °C (Te). Interestingly, the Te of these endotherms was lower than those of NTZ (Figure 4a)

and SAC (Figure 4b), supporting the interpretation that these peaks corresponded to eutectic endotherms as for binary mixtures a lower DSC melting endotherm compared to the parent materials is an indicator of eutectic formation.[15,17,28,29,31] No distinctive depressed DSC melting peaks of excess NTZ or SAC were visualized in Figure 4. However, the shapes of the eutectic endotherms of Figure 4d,e,g looked as they comprised overlapping effects since endothermic shoulders are distinguishable on the right sides of these endotherms (typical of the superposition of two peaks into one peak), and this may be attributed to superposition of *solidus* (eutectic melting) and *liquidus* (melting of the excess of starting material particles) events, as it was observed for other eutectic mixtures.[15,17,31]

Given that the 1:1 PM exhibited a DSC eutectic peak (Figure 4c), other NTZ-SAC physical mixtures (80:20, 60:40, 50:50, 40:60, and 20:80 % w/w) were analyzed, using a melting point apparatus, in order to determine if they also exhibited a eutectic fusion, but we did not attempt to determine the exact eutectic composition[29] due to the thermal decomposition of NTZ and SAC. Only a single invariant *m.p.* (near 176 ºC) was observed in common for the five different compositions prepared (Figure S7). Above the eutectic temperature, the molten phases decomposed, as it was observed in the Kofler hot stage, and this favored the thermal degradation of the remaining solid particles (excess NTZ or SAC). Thus, it is evident that NTZ and SAC are eutectic-forming compounds, and that mechanically induced contact (neat grinding, LAG and even gently mixing) caused eutectic behavior. According to Bi *et al.*,[32] the criteria for eutectic formation are that the eutectic-forming compounds are in intimate contact in solid state and are mutually soluble in each other in the molten state. The intimate contact in the solid state guarantees that eutectic-forming compounds will melt as if a single phase. This contact can be obtained by melting and solidification (which is typically used to form eutectics and its function is only to facilitate the intimate contact between the eutectic-forming compounds;[32] mechanically induced contact, namely compaction that can cause eutectic behavior equivalent to that observed in eutectics formed by fusion,[32] and mechanochemical grinding, which can induce long range

order to give eutectic compositions stabilized by weak, short-range interactions.[29] Evidently, this last method is sufficient to induce the formation of a NTZ-SAC eutectic.

Powder dissolution study under non-sink conditions

The powder dissolution (PD) profiles of 1:1 NTZ-SAC_{LAG} and NTZ (both as dispersed powders sieved through a 100 mesh) obtained in Tween®-t and SLS are shown in Figure 5. The calculated DE values are listed in Table 1.

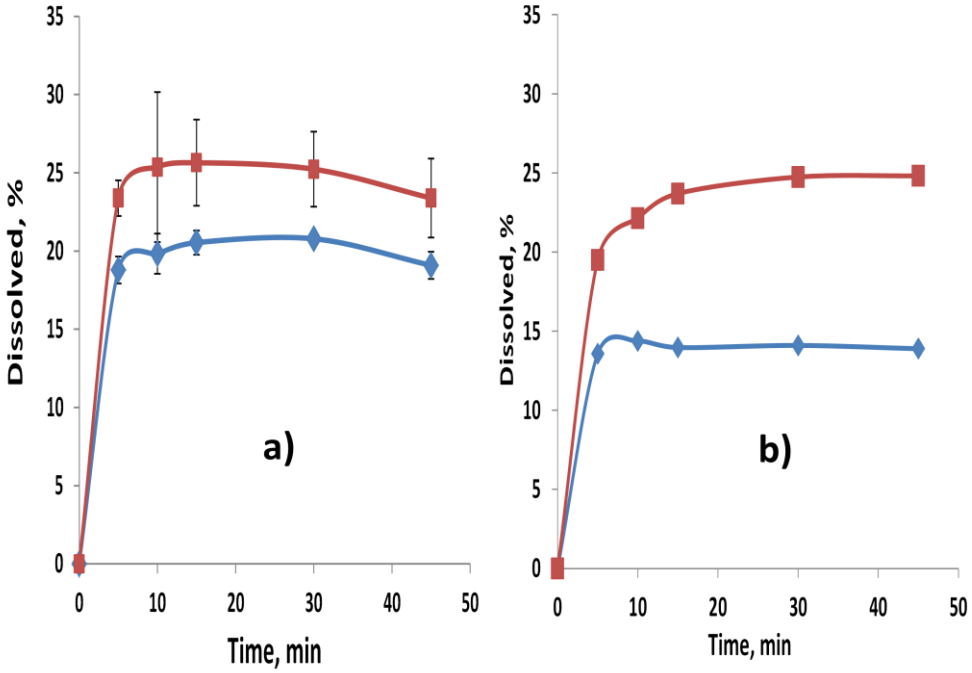

Figure 5. Powder dissolution profiles (USP apparatus 2, 37 ºC ± 0.5 ºC and 75 rpm) of NTZ (filled rhombus) and 1:1 NTZ-SAC_{LAG} (filled squares) in (a) phosphate buffer pH 6.5 with 0.25% Tween® 80 and 0.25 % triethanolamine (*n* =3, error bars indicate the standard deviation), and (b) 0.25% SLS in MilliQ water (*n* =2).

As shown in Figure 5, the dissolution profiles of the 1:1 NTZ-SAC_{LAG} sample were not superimposable to those of pure NTZ neither in Tween®-t nor in SLS, revealing differences in dissolution performance. The DE values for 1:1 NTZ-SAC_{LAG} were slightly higher than those of pure NTZ in the two assayed media (Table 1), indicating that its dissolution process was

more efficient than that of pure NTZ, and the DE advantage ($DE_{NTZ\text{-}SAC}/DE_{NTZ}$) for the NTZ-SAC eutectic was of 1.23 (Tween®-t) and 1.68 (SLS) (Table 1). The small improvement in the dissolution performance of the NTZ-SAC eutectic in comparison to pure NTZ is not surprising when taking into account that SAC is a coformer sparingly soluble in water, which generally enhances the aqueous solubility of drugs when salts (saccharinates) are formed,[13] and small particles of a near-uniform size distribution for NTZ-SAC eutectic were not obtained, namely the samples were sieved only with a standard 100 mesh (150 μm). PD measurements using NTZ-SAC samples with small and narrow particle size distribution (PSD) is a future undertaken given that PD is sensitive to PSD as drug particles are directly exposed to the aqueous solvent and eutectics with small particles and narrow PSC exhibited higher solubility.[15]

Table 1. Dissolution efficiency (DE) for nitazoxanide (NTZ) and 1:1 NTZ-SAC eutectic.

Medium	**DE[a]**		**$DE_{eutectic}$ / DE_{NTZ}**
	NTZ	**1:1 NTZ-SAC_{LAG}**	
Tween® 80-t [b]	19.0	23.4	1.24
SLS[c]	13.2	22.3	1.68

[a] Average values. [b] Phosphate buffer pH 6.5 with 0.25% Tween® 80 and 0.25 % triethanolamine. [c] 0.25% SLS in MilliQ water.

Conclusion

We investigated the capability of NTZ of forming non-covalent interactions with a non-carboxylic acid coformer such as SAC, which cannot form the carboxyl-carboxamidine synthon that has been afforded NTZ cocrystals.[10,11] The screening approach used did not afford cocrystals or salts, as no new unique diffraction lines and signature SSNMR and DRIFT peaks were observed for NTZ-SAC products. However, DSC and HSM revealed that all the NTZ-SAC samples obtained melted at approximately the same temperature (near 176 ºC), which represents

the eutectic reaction of solid NTZ with solid SAC, and demonstrated that NTZ and SAC formed a binary eutectic. Powder dissolution measurements indicated that the NTZ-SAC eutectic (1:1 NTZ-SAC_{LAG}) slightly improved the dissolution performance of NTZ in the two media assayed, and this is an important finding taking into account that SAC is sparingly soluble in water and the NTZ-SAC eutectic did not have a small and near-uniform particle size distribution. Although NTZ did not cocrystallize with SAC, the lack of formation of cocrystals was not a failure of crystal engineering process reactions,[14,16] since it was demonstrated for the first time that NTZ is able to form an eutectic binary mixture with SAC using mechanochemical approaches. Thus, this study enabled to enrich the knowledge about the supramolecular solid-form space of NTZ. Also, this report opens the possibility of preparing new eutectics that might show better dissolution properties than the NTZ-SAC eutectic reported herein, using coformers soluble in water and a green chemistry procedure such as mechanochemistry.

Acknowledgements

This work was supported by SECyT-UNC of Argentina. FPB and OEF are grateful for financial support from CONICET Postdoctoral and Doctoral fellowships, respectively.

Conflict of Interest

The authors declare that they have no conflict of interest.

Supplementary Data

Supplementary file contains Table S1, and Figures S1- S7, and it is available on the journal's web site along with the published article.

References

1. Rossignol J-F. Nitazoxanide: A first-in-class broad-spectrum antiviral agent. Antiviral Res. 2014;10:94-103. doi.org/10.1016/j.antiviral.2014.07.014
2. Chan-Bacab MJ, Hernández-Núñez E, Navarrete-Vásquez G. Nitazoxanide, tizoxanide and a new analogue [4-nitro-N-(5-nitro-1,3-thiazol-2-yl)benzamide; NTB] inhibit the growth of kinetoplastid parasites (*Trypanosoma cruzi* and *Leishmania mexicana*) in vitro. J Antimicrob Chemother. 2009;63:1292-93. doi.org/10.1093/jac/dkp117
3. Mégraud F, Occhialini A, Rossignol J-F. Nitazoxanide, a potential drug for eradication of *Helicobacter pylori* with no cross-resistance to metronidazole. Antimicrob Agents Chemother. 1998:42:2836-40. DOI: 10.1128/AAC.42.11.2836
4. Salas-Zúñiga R, Rodríguez-Ruiz C, Höpfl H, Morales-Rojas H, Sánchez-Guadarrama O, Rodríguez-Cuamatzi P, et al. Dissolution Advantage of Nitazoxanide Cocrystals in the Presence of Cellulosic Polymers. Pharmaceutics. 2020;12:23-40. doi.org/10.3390/pharmaceutics12010023
5. Mahmoud DB, Shitu Z, Mostafa A. Drug repurposing of nitazoxanide: can it be an effective therapy for COVID-19?. J Genet Eng Biotechnol. 2020;18:35. doi.org/10.1186/s43141-020-00055-5
6. DrugBank: nitazoxanide. https://www.drugbank.ca/drugs/DB00507. Accessed 22 March 2020.
7. Gupta Shikhar K, Soni Girish C, Jain SK. Characterization and solubility enhancement of nitazoxanide through β-cyclodextrin inclusion complex. World J Pharm Pharm Sci. 2012; 1:1344-75.
8. Radi AE, Nassef HM, El-Naggar AE. Electrochemical and spectral characterization of the host-guest inclusion complex of the antiparasitic drug nitazoxanide with β-cyclodextrin. Monatsh Chem. 2014;145:421-6. doi.org/10.1007/s00706-013-1109-1

9. Bansal MK, Umashankar MS, Gulati M. Nitazoxanide hard gelatin capsules containing solid dispersions for improving dissolution rate. Inventi Impact: Pharm Tech. 2010(1); inventi:pt/34/10.
10. Félix-Sonda BC, Rivera-Islas J, Herrera-Ruiz D, Morales-Rojas H, Höpfl H. Nitazoxanide Cocrystals in Combination with Succinic, Glutaric, and 2,5-Dihydroxybenzoic Acid. Cryst Growth Des. 2014;14(3):1086-1102. doi.org/10.1021/cg4015916
11. Suresh K, Chaitanya Mannava MK, Nangia A. Cocrystals and alloys of nitazoxanide: enhanced pharmacokinetics. Chem Commun. 2016;52:4223-26. doi.org/10.1039/C6CC00975A
12. Basavoju S, Bostrom D, Velaga SP. Indomethacin–Saccharin Cocrystal: Design, Synthesis and Preliminary Pharmaceutical Characterization. Pharm Res. 2008;25:530-41. doi.org/10.1007/s11095-007-9394-1
13. Banerjee R, Bhatt PM, Ravindra NV, Desiraju GR. Saccharin Salts of Active Pharmaceutical Ingredients, Their Crystal Structures, and Increased Water Solubilities. Cryst Growth Des. 2005;5:2299-2309. doi.org/10.1021/cg050125l
14. Chadha K, Karan M, Chadha R, Bhalla Y, Vasisht K. Is Failure of Cocrystallization Actually a Failure? Eutectic Formation in Cocrystal Screening of Hesperetin. J Pharm Sci. 2017;106;2026-36. dx.doi.org/10.1016/j.xphs.2017.04.038
15. Goud NR, Suresh K, Sanphui P, Nangia A. Fast dissolving eutectic compositions of curcumin. Int J Pharm. 2012;439:63-72. doi.org/10.1016/j.ijpharm.2012.09.045
16. Bala M, Gautam MK, Chadha R. What if Cocrystallization Fails for Neutral Molecules? Screening Offered Eutectics as Alternate Pharmaceutical Materials: Leflunomide-a Case Study. Pharm Sci. 2019;25(3):235-243. doi: 10.15171/PS.2019.46

17. Cherukuvada S, Nangia A. Eutectics as improved pharmaceutical materials: design, properties and characterization. Chem Commun. 2014;50:906-23. doi.org/10.1039/C3CC47521B

18. Delori A, Friščić T, Jones W. The role of mechanochemistry and supramolecular design in the development of pharmaceutical materials. CrystEngComm. 2012;14:2350-62. doi.org/10.1039/C2CE06582G

19. James SL, Adams CJ, Bolm C, Braga D, Collier P, Friščić T, et al. Mechanochemistry: opportunities for new and cleaner synthesis. Chem Soc Rev. 2012;41:413-47. doi.org/10.1039/C1CS15171A

20. Weyna DR, Shattock T, Vishweshwar P, Zaworotko MJ. Synthesis and Structural Characterization of Cocrystals and Pharmaceutical Cocrystals: Mechanochemistry vs. Slow Evaporation from Solution. Cryst Growth Des. 2009;9:1106-23. doi.org/10.1021/cg800936d

21. Bruno FP, Caira MR, Monti GA, Kassuha DE, Sperandeo NR. Spectroscopic, thermal and X-Ray structural study of the antiparasitic and antiviral drug Nitazoxanide. J Mol Struct. 2010;984:51-7. doi.org/10.1016/j.molstruc.2010.09.006

22. Romañuk CB, Manzo RH, Linck YG, Chattah AK, Monti GA, Olivera ME. Characterization of the solubility and solid-state properties of saccharin salts of fluoroquinolones. J Pharm Sci. 2009;98(10):3788-3801. doi.org/10.1002/jps.21688

23. Yugeng Z. Spectral and thermal properties of saccharin and saccharin metal complexes. Transition Met Chem. 1994;19:446-48. doi.org/10.1007/BF00139325

24. Zoeller T, Klein S. Simplified Biorrelevant Media for Screening Dissolution Performance of Poorly Soluble Drugs. Dissolution Technol. 2007:14(4):8-13. dx.doi.org/10.14227/DT140407P8

25. Malesuik MD, Cardoso SG, Steppe M. Development of a Validated Stability-Indicating LC Method for Nitazoxanide in Pharmaceutical Formulations. Chromatographia. 2008;67:131-6. doi.org/10.1365/s10337-007-0454-9

26. Rossi RC, Dias CL, Donato EM, Martins LA, Bergold AM, Fröehlich PE. Development and validation of dissolution test for ritonavir soft gelatin capsules based on in vivo data. Int J Pharm. 2007;338:119-24. doi: 10.1016/j.ijpharm.2007.01.036

27. Khan KA. The concept of dissolution efficiency. J Pharm Pharmacol. 1975;27:48-9. doi.org/10.1111/j.2042-7158.1975.tb09378.x

28. Fandiño OE, Reviglio L, Garro Link Y, Monti GA, Marcos Valdez MM, Faudone SN, et al. Novel cocrystals and eutectics of the antiprotozoal tinidazole: mechanochemical synthesis, cocrystallization and characterization. Cryst Growth Des. 2020;20(5):2930-42. doi.org/10.1021/acs.cgd.9b01435

29. Cherukuvada S, Guru Row TN. Comprehending the Formation of Eutectics and Cocrystals in Terms of Design and Their Structural Interrelationships. Cryst Growth Des. 2014;14:4187-98. dx.doi.org/10.1021/cg500790q

30. Matsuoka M, Ozawa R. Determination of solid-liquid phase equilibria of binary organic systems by differential scanning calorimetry. J Cryst Growth. 1989;96:596-604. doi.org/10.1016/0022-0248(89)90057-2

31. Gorniak A, Wojakowska A, Karolewicz B, Pluta J. Phase diagram and dissolution studies of the fenofibrate–acetylsalicylic acid system. J Therm Anal Calorim. 2011;104:1195-1200. doi.org/10.1007/s10973-010-1148-3

32. Bi M, Hwang S-J, Morris KR. Mechanism of eutectic formation upon compaction and its effects on tablet properties. Thermochim Acta. 2003;404:213-26. doi.org/10.1016/S0040-6031(03)00185-0

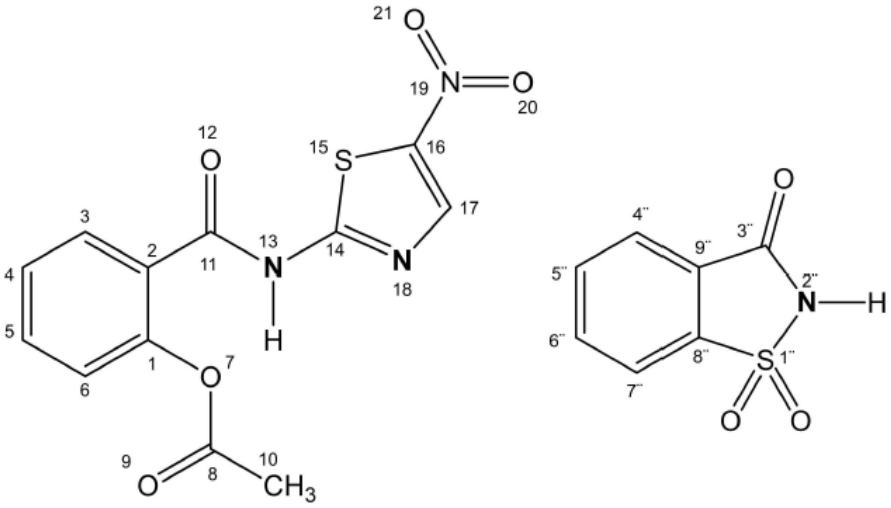

Figure 1. Schemes of the molecules of nitazoxanide (NTZ) and saccharine (SAC), and atom numbering used in the SS 13C NMR study for NTZ and SAC.

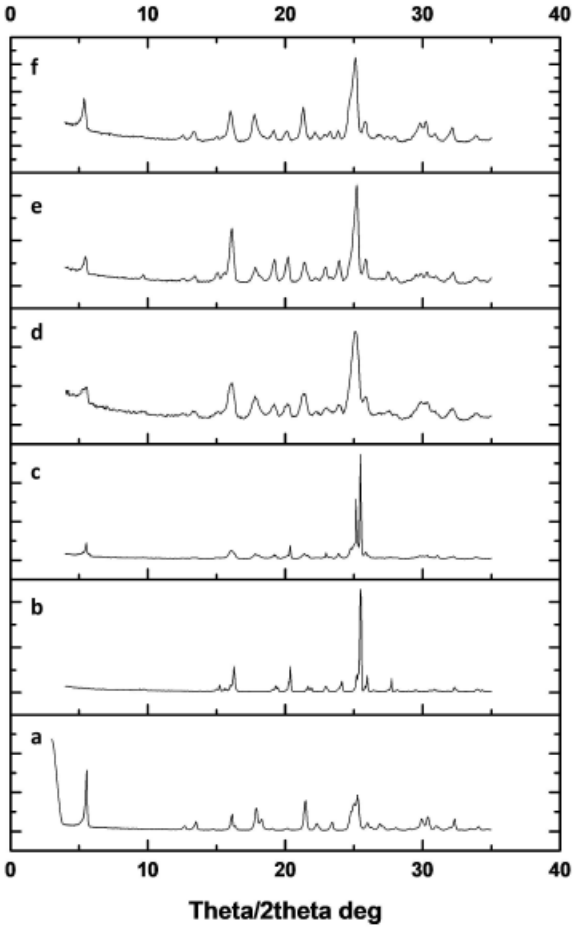

Figure 2. X-ray powder diffraction patterns of (a) NTZ; (b) SAC; (c) 1:1 PM; (d) 1:1 NTZ-SACLAG; (e) 1:2 NTZ-SACLAG, and (f) 2:1 NTZ-SACLAG.

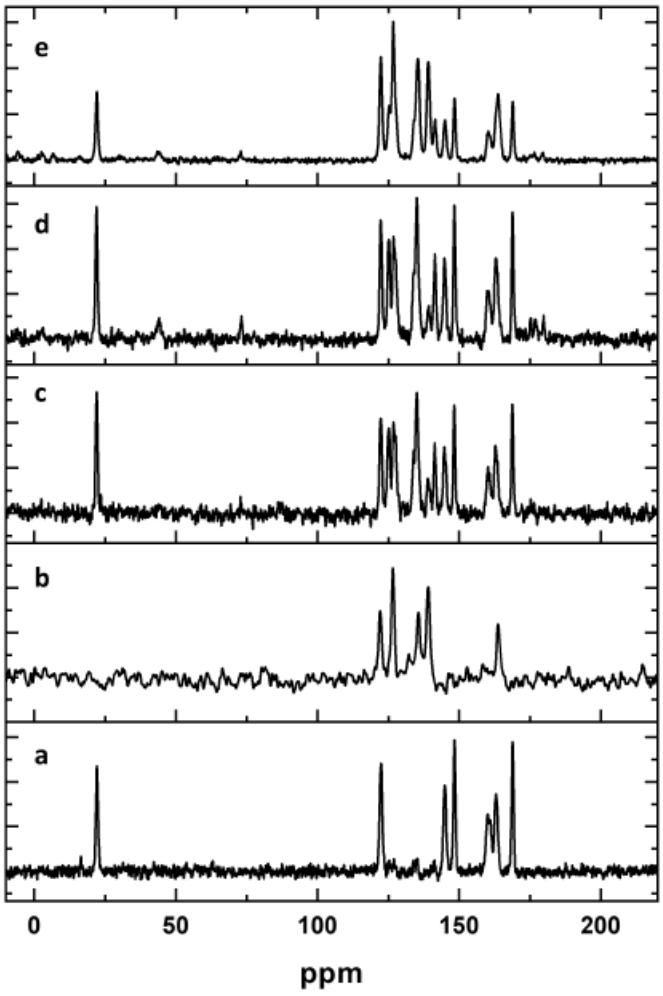

Figure 3. 13C CPMAS NMR spectra of (a) NTZ; (b) SAC; (c) 1:1 PM; (d) 1:1 NTZ-SACNG, and (e) 1:2 NTZ-SACLAG.

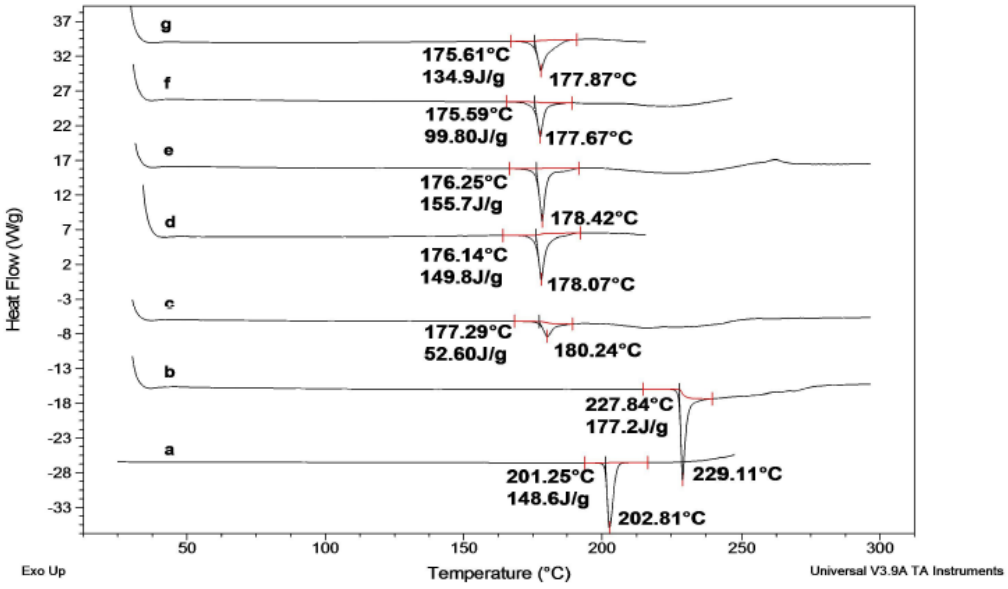

Figure 4. DSC (non-hermetically sealed aluminum pans, β = 10 °C/min and N2 purge of 50 mL/min) of (a) NTZ; (b) SAC; (c) 1:1 PM; (d) 1:1 NTZ-SACNG; (e) 1:2 NTZ-SACNG; (f) 1:2 NTZ-SACLAG, and (g) 2:1 NTZ-SACNG.

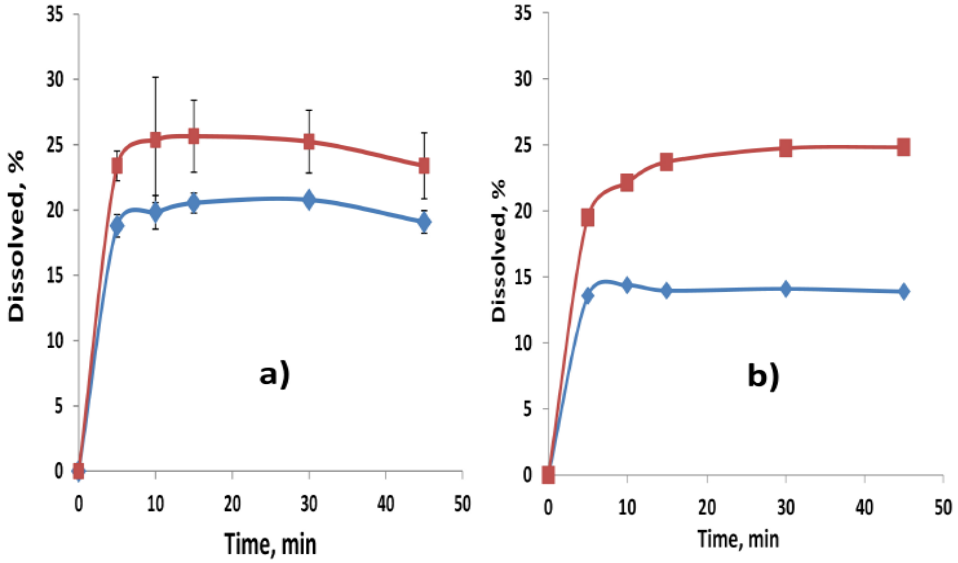

Figure 5. Powder dissolution profiles (USP apparatus 2, 37 ºC □ 0.5 ºC and 75 rpm) of NTZ (filled rhombus) and 1:1 NTZ-SACLAG (filled squares) in (a) phosphate buffer pH 6.5 with 0.25% Tween□ 80 and 0.25 % triethanolamine (n =3, error bars indicate the standard deviation), and (b) 0.25% SLS in MilliQ water (n =2).